Nanostructured Rh/SiC@SiO2 core@shell catalysts for microwave-assisted dry reforming of methane

Palomo, José; Caspers, Max; Urakawa, Atsushi

DOI
10.1016/j.cattod.2025.115464

Publication date
2025

Document Version
Final published version

Published in
Catalysis Today

Catalysis Today 460 (2025) 115464

Contents lists available at ScienceDirect

Catalysis Today

journal homepage: www.elsevier.com/locate/cattod

Nanostructured Rh/SiC@SiO_2 core@shell catalysts for microwave-assisted dry reforming of methane

José Palomo, Max Caspers, Atsushi Urakawa *

Catalysis Engineering, Chemical Engineering Department, Delft University of Technology, Van der Maasweg 9, Delft 2629 HZ, the Netherlands

ARTICLE INFO

Keywords:
Core-shell
DRM
Microwave-assisted reactor
Nanostructured catalysts

ABSTRACT

Dry reforming of methane (DRM) was investigated using nanostructured core@shell materials, thermally activated with two different heating methods, namely conventional resistive heating and microwave. The core@shell catalysts were composed of β-SiC nanoparticles, with a mean particle size below 100 nm, coated by a uniform SiO_2 shell of ca. 30 nm thickness. Highly dispersed Rh nanoparticles, with a mean particle size of 2.5 nm, were present on the surface of the SiO_2 shell. Operation under microwave heating conditions enhanced the reverse water gas shift reaction activity, which takes place in parallel with the DRM process, as compared to the operation under resistive heating conditions. Moreover, stable long-term operation was achieved under microwaved-assisted conditions, due to the unique spatial arrangement of the phases composing the nanostructured catalytic system, together with the suppression of irreversible coke deposition.

1. Introduction

Despite efforts to seek cleaner energy alternatives, fossil fuels remain the primary energy source. Among them, natural gas – comprising 85–99 % methane (CH_4) – is receiving a great deal of attention as a feedstock. Besides, with the new reserves discovered annually, alongside a growing emphasis on shale gas extraction, its availability will remain high in the near future [1,2].

At present, only 15 % of natural gas is used as a feedstock, primarily for hydrogen and syngas production [3]. The remaining is burned for heating and electricity generation [4], accounting for 22 % of global CO_2 emissions [5]. Given the inevitable decline in natural gas combustion over the years, research into existing and emerging methane-based feedstock processes is becoming increasingly relevant in the context of the energy transition.

The limited use of methane as a chemical feedstock arises from the challenge of activating its stable, non-polar C-H bonds, which requires the use of catalysts and harsh conditions to achieve practical methane conversions, making these processes highly energy-intensive [6]. Current industrially relevant methane transformation relies on steam reforming of methane (SRM), which yields syngas, a CO and H_2 mixture used in ammonia, methanol, and hydrocarbon production [4,7]. However, this process is highly energy-intensive due to its endothermic nature, requiring superheated steam and temperatures above 800–900 °C, leading to high operational costs [1,4,7]. On the other hand, dry reforming of methane (DRM) (Eq. (1)) has been widely explored as an alternative to SRM for syngas production. DRM uses CO_2 instead of H_2O to oxidize CH_4, which makes this process highly relevant with the growing focus on CO_2 utilization [8]. By utilizing CO_2, syngas production could become more sustainable, especially with advancing CO_2 capture technologies [9].

$$CH_4 + CO_2 = 2H_2 + 2CO \quad \Delta H^{\circ}_{298K} = 247 kJ/mol \tag{1}$$

Nevertheless, this reaction is also highly endothermic, typically requiring temperatures of 700–1000 °C, making it an energy-intensive process. Active catalysts, mainly rhodium-based [10] and nickel-based [11], have been reported in literature. Several studies revealed that irreversible coke deposition and, consequently, catalyst deactivation is one of the main issues hindering the industrial implementation of the DMR process [1,8,12,13]. On the other hand, efficient reactor heating is crucial for DRM to control heat transfer and minimize energy consumption due to its high energy demands. In this context, microwave-assisted methane conversion emerges as a promising alternative to conventional heating [7,14,15].

Microwave heating, as opposed to conventional heating, offers higher heating rates and selective catalyst bed heating, creating a gas-solid temperature gradient which can reduce unwanted side reactions [7,14,16]. Additionally, microwave heating is believed to mitigate

* Corresponding author.
A.Urakawa@tudelft.nl (A. Urakawa)

https://doi.org/10.1016/j.cattod.2025.115464
Received 24 April 2025; Received in revised form 31 May 2025; Accepted 13 July 2025
Available online 18 July 2025

coke-induced catalyst deactivation, as coke is microwave-susceptible and can be selectively thermally targeted for removal [17,18].

Most of catalyst support materials for DMR are microwave-transparent. Therefore, catalysts must be modified for compatibility with microwave reactors [7]. This involves incorporating microwave-susceptible materials into the reactor to ensure a suitable microwave absorption capacity by the catalyst bed. Physically mixing conventional catalysts with microwave-susceptible materials has been shown to enable sufficient microwave absorption, achieving the necessary reaction temperatures for DRM operation [9]. This approach also improved conversion and yield compared to conventional heating [14]. However, inhomogeneous mixing could lead to local hot and cold spots, posing a challenge for uniform heating [2,9].

To tackle this challenge, the use of structured catalysts in which a microwave-susceptible material is implemented in the catalyst bed has been proposed [2,7,15,17]. One of the spatial arrangements that could enhance the microwave-susceptible material and the catalyst phase interaction is the core@shell structure, with a microwave-susceptible core and a support shell hosting the metal active sites for DRM.

In this way, microwave heating raises the core temperature, which then transfers heat to the shell via conduction. Unlike conventional heating, the gas phase is not directly heated, transferring heat first by diffusion from the solid to the gas, which is transported to affect the temperature of the downstream positions by convection, resulting in a lower average gas temperature. Core@shell structures have been successfully used in other methane activation processes such as the oxidative coupling of methane, demonstrating their effectiveness in achieving uniform temperature distribution [2].

Silicon carbide (SiC) is a promising core material due to its strong microwave absorption capacity, high thermal conductivity, and chemical inertness [9]. However, its inertness makes its coating challenging. Research on SiC core@shell structures has mainly focused on silicon oxide (SiO_2) shells for their compatibility and high surface area [19–21]. SiC@SiO_2 materials have been synthesized for use outside of catalysis using a modified Stöber process, where Tetraethyl orthosilicate (TEOS) hydrolyzes in alcohol with ammonia as a catalyst [22]. This same method can coat SiC by hydrolysing TEOS on its surface, requiring silane coupling agents for SiC [23,24].

Given the benefits of core@shell catalysts in microwave reactors for oxidative coupling of methane, investigating their potential for other methane transformation processes presents a valuable research opportunity. This study therefore aims to contribute to reducing this research gap by investigating SiC@SiO_2 as core@supports for DRM catalysts.

In this work, we explore the preparation of nanostructured core@shell catalysts, with enhanced microwave absorption properties, for DRM. The catalysts were synthesized by coating microwave-susceptible β-SiC nanoparticles via a modified Stöber method with SiO_2, followed by Rh impregnation. DRM was investigated using the nanostructured Rh/SiC@SiO_2 materials, thermally activated with two different heating methods, namely conventional resistive heating and microwave.

2. Experimental method

2.1. Materials

Ethanol (Absolute, ≥ 99.8 %, Honeywell), Pluronic F-127 (Sigma-Aldrich), Ammonium hydroxide solution (ACS Reagent, 28–30 % NH_3 basis, Sigma-Aldrich), Tetraethyl orthosilicate (TEOS) (99.999 % trace metal basis, Sigma-Aldrich), and SiC (beta phase, 45–55 nm, Thermo Scientific Chemicals) were used for the synthesis of the core@shell supports. Rhodium(III)chloride anhydrous, (3-Aminopropyl)triethoxysilane (≥ 98 %, Merck Sigma), and Sodium borohydride (ReagentPlus, 99 %, Sigma-Aldrich) were used for the metal loading. Milli-Q water was used throughout the experiments.

2.2. Catalyst preparation

SiC@SiO_2 support was prepared using a modified Stöber method, based on the procedure reported by Zhang et al. [23], with the difference of using SiC instead of Fe_3O_4 and the addition of a prior step of dispersing Pluronic F-127 before adding the core material. Pluronic F-127 acts as a surfactant and facilitates the formation of the shell layer [25].

20 mg of Pluronic F-127 was dissolved in a solution of 180 mL ethanol and 12 mL water by ultrasonication for 30 min. Next, 0.2 g of nano-sized SiC was added to the solution, and the dispersion was sonicated for 30 min. Afterwards, 6 mL of 30 wt% ammonia solution was added. The mixture was stirred for 5 min using an overhead stirrer, after which 600 μL of TEOS was added. The reaction mixture was then stirred for 17 h at room temperature. The resulting mixture was centrifuged for 10 min at 6000 rpm, followed by removing the supernatant. The solid material was then washed once with water and once with ethanol, again utilizing centrifugation followed by removal of the supernatant liquid, and dried at 60 °C overnight. The uncalcined support was denoted as SiC@SiO_2-U. Part of the dried material was calcined at 600 °C for 4 h under static air conditions. This sample was denoted as SiC@SiO_2. Based on gravimetric analyses, the SiO_2 wt% was estimated to be 35 %.

2.5 wt% Rh was loaded on the core@shell supports using the method reported by Liu et al. [26]. 0.5 g of the uncalcined core@shell support (SiC@SiO_2-U) and 375 μL of 3-(aminopropyl)-triethoxysilane (APTS) were dissolved in 175 mL pure isopropyl alcohol. The reaction mixture was vigorously stirred for 8 h at 70 °C in an oil bath. A condenser was fitted around the overhead stirrer's shaft to minimize solvent loss. The solid material was recovered by centrifugation, washed twice with water, and dried at 60 °C for 4 h under vacuum. The functionalized support was denoted as SiC@SiO_2-APTS.

In a second step, 0.4 g of SiC@SiO_2-APTS and 11 mg of Rh chloride were dissolved in 100 mL of ethanol by ultrasonication for 30 min. Afterwards, 50 mL of 0.14 mol/L $NaBH_4$ solution was added to the mixture and left to react for 2 h at room temperature using an overhead stirring. The resulting solid material was collected through centrifugation, washed twice with water, and dried at 60 °C for 4 h under vacuum conditions. Finally, the catalyst was heat-treated in a muffle furnace at 600 °C for 4 h under static air conditions. This material was denoted as Rh/SiC@SiO_2.

2.3. Characterization of the catalysts

The morphology of the core@shell materials was studied by transmission electron microscopy. TEM images were acquired in a JEOL JEM-1400plus instrument.

The porous texture of the materials was characterized by N_2 physisorption at − 196 °C, performed in a Tristar II 3020 equipment (Micromeritics). Samples were previously outgassed under vacuum overnight at 150 °C. From the N_2 adsorption-desorption isotherm, the apparent surface area (A_{BET}) was determined by applying the BET equation [27].

X-ray diffraction patterns (XRD) of the prepared materials were recorded on a Bruker D8 Advance X-ray diffractometer using Co-Kα radiation (λ = 0.15406 nm), at a scan step of 0.02°/s in the region between 10 and 90°. All patterns were background-subtracted to eliminate the contribution of air scatter and possible fluorescence radiation.

The carbon content in the spent samples was determined by thermogravimetric analyses (TGA), which were carried out using a Mettler Toledo TGA/SDTA851e instrument. Samples were heated from room temperature to 800 °C, at a heating rate of 5 °C/min under continuous synthetic air flow (100 cm^3_{STP}/min).

2.4. Catalytic experiments

Catalytic experiments were carried out under conventional resistive

heating (RH) and under microwave radiation heating (MW) conditions, using a customized laboratory-scale, continuous flow reaction system provided with a quartz fixed bed microreactor (i.d. 4 mm). For resistive heating experiments, the reaction temperature was measured and controlled with a K-type thermocouple inserted at the end of the catalyst bed. For microwave-assisted heating experiments, Ryowa electronics (2.45 GHz ± 50 MHz, maximum 100 W) microwave device was used. The temperature of the catalyst was monitored by a one-point IR temperature sensor, and the resonance frequency of microwaves inside the cavity was measured by the detector. With the feedback of these two parameters, the heating power and thus the catalyst temperature was controlled.

In a typical experiment, the catalyst (pelletized to a 200–300 μm particle size) was loaded in the quartz reactor and fixed with quartz wool. Prior to starting the reaction, the catalyst was in situ reduced at 600 °C, under a constant flow of 20 % H_2 in helium (50 mL/min), for 30 min. Once carried out the reduction stage, the temperature was set to the reaction value, and the gases were introduced. The reaction mixture consisted of CH_4 (25 vol%), CO_2 (25 vol%), He (40 vol%), and N_2 (10 vol%). The space velocity was set as 3000 $mL_{gas}/(g_{cat}$ min). The outlet gas concentrations were analyzed by gas chromatography (GC, Agilent 7890B, equipped with two FIDs and one TCD). N_2 was used as an internal standard for GC analyses.

CH_4 and CO_2 conversions were defined as the ratio of the amount of CH_4 or CO_2 converted to the amount of the specific reactant (CH_4 or CO_2) supplied to the reactor and were expressed in molar %. The H_2 to CO ratio was calculated as the molar flow of H_2 divided by the molar flow of CO at the reactor outlet.

3. Results and discussion

3.1. Characterization results

The morphology of the core@shell materials was examined by transmission electron microscopy (TEM). Fig. 1 shows a collection of TEM images of the $SiC@SiO_2$ and $Rh/SiC@SiO_2$ samples. These images confirmed the successful preparation of the intended core-shell structure for both the catalyst support and the final catalyst. A high uniformity in terms of silica coating on the SiC nanoparticles is observed, with a shell thickness in the range of 25–30 nm, which is in line with the findings reported by Zhang et al. [23]. After the Rh loading stage, the core@shell morphology of the material remained unaltered, with the incursion of very well dispersed Rh nanoparticles on the surface of the SiO_2 shell. The Rh particle size was highly uniform with a mean particle size of 2.5 nm. This mean Rh particle size value is considerably lower than those reported in other studies on Rh-supported catalysts based on SiC-SiO_2 composites. In this regard, Petersen et al. [28] reported the preparation of Rh-SiC/SiO_2 catalysts through high-temperature oxidation of SiC, followed by Rh loading via wetness impregnation, which resulted in a Rh mean particle size of 10–20 nm. On the other hand, the results presented here in terms of Rh particle size are in line with the findings reported by Liu et al. [26], who also observed a high Rh dispersion on $Rh/Fe_3O_4@SiO_2$ nanostructured core@shell catalysts prepared through a similar procedure. However, it is worth mentioning that, in the present study, the samples underwent a calcination stage at 600 °C. These findings indicate that the materials reported in the present study exhibit high thermal stability, making them highly attractive for high-temperature catalysis applications.

The porous texture of the nanostructured materials was analyzed by N_2 adsorption-desorption at − 196 °C. Fig. 2 presents the N_2 adsorption-desorption isotherms of the samples. The core material, SiC nanoparticles, presented a type II isotherm, with a very low nitrogen adsorption in the whole range of relative pressures, which is characteristic of nonporous materials [29]. The specific surface area calculated for this sample was estimated using the BET equation, and a value of 28 m^2/g was obtained. Once silica coated, the resulting material, $SiC@SiO_2$, exhibited an increase in the adsorbed nitrogen, especially at the low relative pressure range, suggesting the presence of micropores in the structured material. The BET surface area calculated for this sample showed a value of 50 m^2/g, which reflects an increase of specific surface area of almost twice the value of the core material itself. Considering that the core material accounts for 65 % of the total $SiC@SiO_2$ weight, these results further indicate that the silica shell coating has a well-developed porous texture, which could contribute to the high Rh dispersion achieved in the final core@shell catalyst. The pore size distribution of this core@shell support is presented in Fig. S1. After Rh loading, $Rh/SiC@SiO_2$, the N_2 uptake experienced a decrease, with a corresponding decrease in the BET surface area up to a value of 19 m^2/g, which suggested that the micropores initially present in the core@shell support ($SiC@SiO_2$), were filled/blocked by the metal nanoparticles deposited during the impregnation stage.

X-ray diffraction patterns of the samples are shown in Fig. 3. The XRD pattern of the core material confirmed the existence of only the β-SiC crystal phase (PDF73-1665). Upon silica coating, a broad peak at 2θ = 20–30° was observed, which could be attributed to amorphous SiO_2. These results align well with the observations made by TEM, where no crystalline arrangement was detected for the silica shell. This

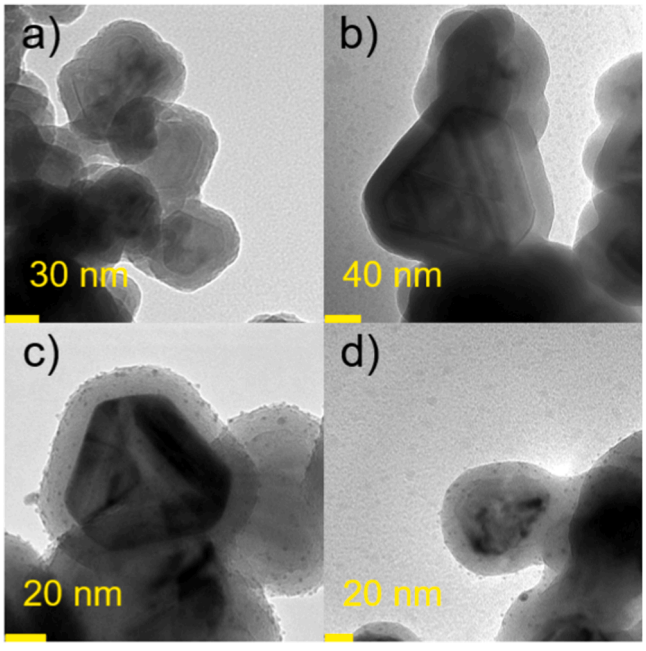

Fig. 1. TEM images of a) and b) $SiC@SiO_2$ calcined, c) fresh $Rh/SiC@SiO_2$, and d) $Rh/SiC@SiO_2$ after reaction at 800 °C.

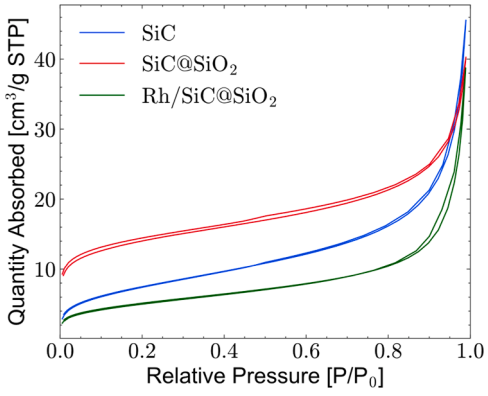

Fig. 2. Nitrogen adsorption–desorption isotherms at − 196 °C of the structured materials.

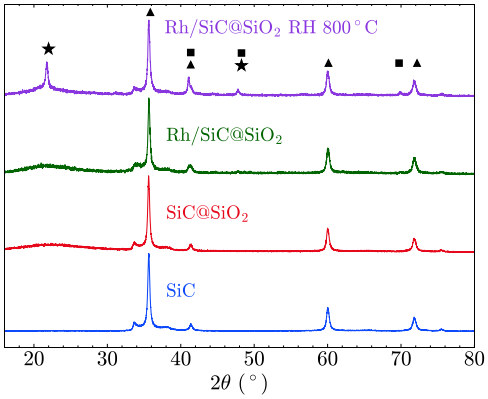

Fig. 3. XRD of the bare core and the structured materials. SiO_2 (★), SiC (▲), Rh (■).

amorphous structure was maintained even after calcination at 600 °C (see $SiC@SiO_2$ in Fig. 3). The XRD pattern of the $Rh/SiC@SiO_2$ catalyst displayed the same diffraction peaks as the support, with no diffraction peaks corresponding to Rh crystalline phases. This suggested that the crystallite sizes of the Rh particles are below the detection limit of the instrument and/or they are present in an amorphous phase.

3.2. Catalytic experiments and characterization of the spent samples

The Rh-containing core@shell catalyst, $Rh/SiC@SiO_2$, was used to promote the dry reforming of methane (DRM) reaction. Fig. 4 shows the DRM performance as a function of the temperature for resistive heating operation conditions. As expected, CH_4 and CO_2 conversion exhibited an increase with rising reaction temperature, reaching values of 74 and 82 %, respectively, at 800 °C. The higher CO_2 than CH_4 conversion values, in all temperature ranges, indicated the occurrence of the reverse water-gas shift (RWGS) reaction as a side reaction [30,31]. This reaction consumes part of the generated H_2 by reacting with CO_2, producing further CO and water. The occurrence of the RWGS reaction was also evident from the H_2/CO ratio, which showed a value lower than one within the whole temperature range. Attending to the evolution of this reaction index with temperature, it could be seen that, even though higher reaction temperatures promote RWGS, the increase in the H_2/CO ratio with rising reaction temperature indicated that the DRM process prevailed over RWGS at higher temperatures, which is in line with previous studies reported in literature [32].

The spent catalyst was characterized after DRM operation at 800 °C. TEM analyses (see Fig. 1d) showed that, even after these harsh operation conditions, the Rh nanoparticles remained evenly distributed within the SiO_2 shell. On the other hand, TEM images suggest a slight increase in particle size; nevertheless, measurements still indicate a 2–6 nm Rh particle diameter. Besides, the apparent reduction in the number of individual Rh particles was attributed to the sintering of the very small Rh nanoparticles. The XRD pattern of the spent catalyst is shown in Fig. 3. This pattern evidenced the presence of metallic Rh crystalline phases, with diffraction peaks appearing at $2\theta = 42°$ and 48° (PDF#05-0685). The presence of these diffractions could indicate the formation of larger Rh nanoparticles due to sintering at high temperature. Nevertheless, these larger particles were not detected in TEM to a large extent, indicating that the majority of the Rh nanoparticles were still in a very small particle size. Moreover, the Rh crystal size could not be effectively determined due to the overlapping of the diffraction peaks with the other phases present in the structured materials. On the other hand, it could also be seen that diffraction peaks related to SiO_2 crystalline phases became significantly sharper for the spent catalyst. A closer inspection revealed the formation of a cristobalite crystalline phase (PDF82-0512). Amorphous silica typically crystallizes at higher temperatures than 800 °C (e.g. 1000–1200 °C) [33,34]. The crystallisation at lower temperature observed in the present study can be attributed to the nano-size of the silica shell and subsequent higher surface area compared to bulk amorphous silica.

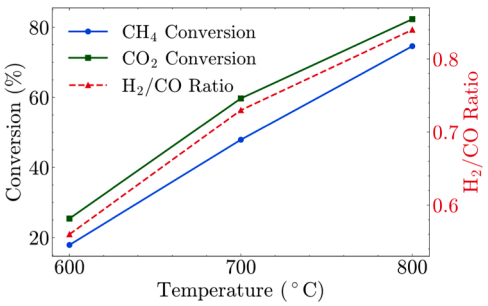

Fig. 4. CH_4 and CO_2 conversion, and H_2:CO ratio for $Rh/SiC@SiO_2$.

The nanostructured core@shell material prepared here was also evaluated as potential catalyst for the DRM reaction under microwave-assisted heating conditions. The effect of the heating method (resistive and microwave-assisted heating) on the catalytic performance and stability with time on stream of the catalyst was analyzed. In order to clearly observe the stability with time on stream features of the catalyst, the operation conditions were set aiming that the attained CH_4 and CO_2 conversions were significantly lower than the thermodynamic equilibrium. It is also worth mentioning that the $Rh/SiC@SiO_2$ catalyst prepared in this study showcased sufficient microwave absorption capacity so as to be heated up to the reaction temperature without the addition of any further microwave absorbing material into the catalyst bed.

Fig. 5 shows the catalytic performance, in terms of CH_4 and CO_2 conversions and H_2/CO ratio as a function of time on stream, at 600 °C, for resistive heating (RH) and microwave-assisted heating (MW) conditions. CO_2 conversion presented similar values for both of the heating

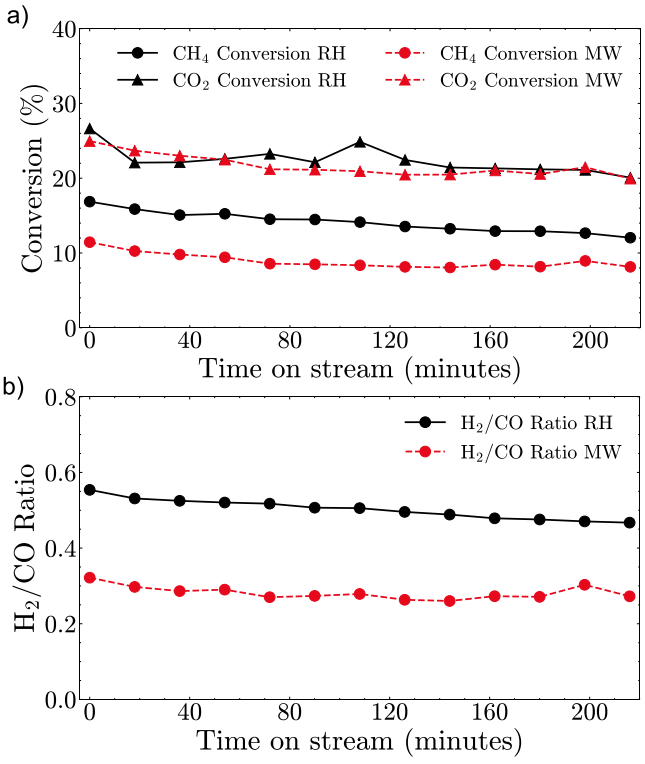

Fig. 5. CH_4 and CO_2 conversion, and H_2:CO ratio as a function of time on stream at 600 °C for $Rh/SiC@SiO_2$, under resistive heating (RH) and microwave-assisted (MW) heating conditions.

methods. However, CH_4 conversion value was significantly lower in the case of MW heating conditions. On the other hand, the H_2/CO ratio presented a lower value in the case of the operation under MW conditions. DRM process has been reported to proceed in two steps [35], namely: i) the methane decomposition reaction, yielding carbon and H_2 (Eq. (2), and ii) the gasification of the carbon deposits by CO_2, yielding CO (Eq. (3). This mechanism runs in parallel with the occurrence of the RWGS reaction (Eq. (4)).

$$CH_4 = 2H_2 + C \quad \Delta H^{\circ}_{298K} = 74.9 kJ/mol \tag{2}$$

$$C + CO_2 = 2CO \quad \Delta H^{\circ}_{298K} = 172.4 kJ/mol \tag{3}$$

$$H_2 + CO_2 = H_2O + CO \quad \Delta H^{\circ}_{298K} = 41 kJ/mol \tag{4}$$

The results obtained here pointed out that operating under microwave-assisted heating conditions led to a lower extent of methane cracking (Eq. (2), which suggested less carbon deposits on the catalyst surface susceptible to be gasified by CO_2 (Eq. (3)). On the other hand, the CO_2 conversion turned out to be almost the same for both heating methods. This similarity in this reaction index, along with the lower H_2/CO ratio observed under microwave heating conditions, clearly evidenced that the RWGS reaction was enhanced under operating with this heating method. This higher activity towards the RWGS reaction could be attributed to the unique heating properties of MW, with the possible generation of localized hotspots that could exacerbate this side reaction. Regarding the stability, differences could also be appreciated when comparing both heating methods. The catalytic results obtained under RH conditions evidenced a continuous deactivation of the catalyst with time on stream, especially related to the methane activation features. In this sense, CH_4 conversion experienced a gradual decrease, passing from 17 to 12 % after 3.5 h on stream, and without reaching a pseudo steady-state operation. This decrease in methane conversion, under RH conditions, could be related to the formation of highly stable carbon deposits, which could not be fully in situ gasified by CO_2, yielding the deactivation of part of the active sites of the catalyst due to the irreversible coke deposition. Besides, the decrease in CH_4 decomposition activity was accompanied by a slight decrease in the H_2/CO ratio (see Fig. 5b), which could also indicate that under these conditions, where carbon deposits could present some limitations towards their full gasification, the RWGS reaction got favored as route for the conversion of CO_2. On the other hand, operation under MW heating conditions yielded a stable catalytic performance, with only a slight decrease in methane conversion from 11 to 8 % in the first 80 min of reaction, and remaining all the reaction indexes stable with time on stream from this time onwards. More severe operation conditions, i.e., higher concentration of reactants, and higher temperatures, were also set to evaluate the stability of this catalytic system under both conventional and microwave heating, with the results also showing a high stability with time on stream (see Fig. S2). These results clearly highlight that the engineering of catalysts in this core@shell conformation at the nanometric scale is a highly effective strategy for developing a catalytic system with suitable microwave absorption properties and with enhanced stability with time on stream.

The spent catalysts, after stability with time on stream at 600 °C experiments, were also analyzed. XRD patterns obtained for the catalyst after DRM reaction under both heating method conditions are shown in Fig. 6, together with the fresh catalyst, for comparison purposes. The presence of metallic Rh crystalline phases was detected for both of the spent samples, with diffraction peaks appearing at a $2\theta = 42°$ and 48° (PDF05-0685). The intensity and broadness of the aforementioned peaks presented similar intensities and broadness, with a slight increase in the sharpness for the case of MW heating operation. As previously discussed, the Rh crystal size could not be effectively calculated due to the overlapping of the diffraction peaks with those belonging to the other crystalline phases present in the structured material. On the other hand, a significant difference was observed in relation to the crystalline

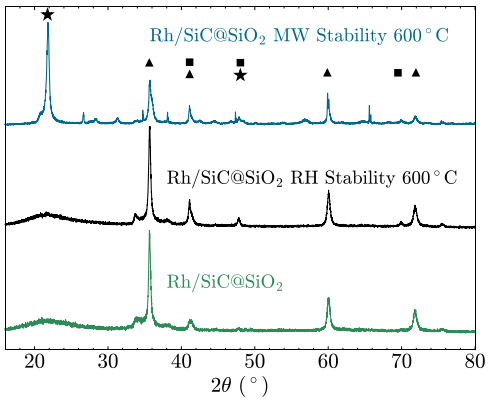

Fig. 6. XRD for Rh/SiC@SiO_2, catalyst before and after reaction at 600 °C, under resistive heating and microwave-assisted heating conditions. SiO_2 (★), SiC (▲), Rh (■), quartz (●).

structure of the silica shell. In the case of RH operation, the silica structure was not significantly altered as compared to the fresh catalyst, maintaining its original amorphous phase. Conversely, intense crystallite peaks corresponding to cristobalite crystalline phase (PDF82-0512) were observed for the catalyst used under MW heating DRM. A similar phase transformation was observed for the catalyst that was operating at 800 °C under RH conditions (see Fig. 3d). This phase transformation at lower set point temperature in the case of MW operation could be attributed to the unique heating features of microwaves, with a very localized heating character [36]. In this sense, the core material SiC, being a well-known microwave absorbing material, is likely to be reaching a higher temperature than the outer SiO_2 shell of the catalyst, which is microwave transparent, and, therefore, the SiC-SiO_2 interphase could also be at a higher local temperature compared to the outer shell of the catalyst. This localized increase in temperature could be an explanation for the slight sharpening of the Rh diffraction peaks observed for the spent catalyst operated under MW heating conditions.

Thermogravimetric analyses (TGA) were also performed on both of the spent catalysts (i.e., after the different heating method operation), after 4 h of DRM reaction at 600 °C, and the results are presented in Fig. 7. Despite the relatively short reaction times, striking differences when comparing both heating methods were observed. The catalyst submitted to RH operating conditions showed a mass loss starting at a temperature around 450 °C, which was associated with the oxidation of disordered carbon deposits [37]. The presence of these carbon deposits is in line with the catalytic observations, in which a decrease in methane conversion as a function of time was observed (See Fig. 5), further suggesting coke deposition on the active Rh phase of the catalytic system as the main cause for catalyst deactivation, as also reported for other

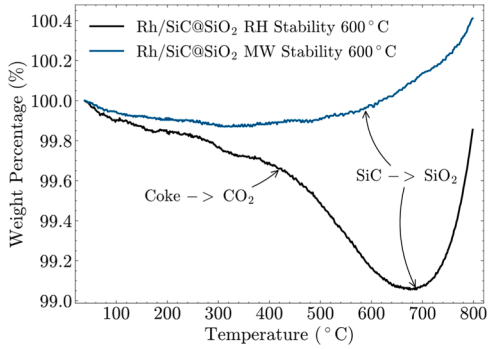

Fig. 7. TGA profiles for Rh/SiC@SiO_2 after reaction at 600 °C, under resistive heating and microwave-assisted heating conditions. The increase in weight above 700 °C is associated with the oxidation of the SiC core material.

catalyst in literature [38]. In contrast, the spent catalyst after operation under MW heating conditions did not show any weight loss during TGA analyses, indicating the absence of coke deposits in this catalyst. The lower carbon accumulation observed for MW heating operation was attributed to both the lower methane decomposition reaction extent and also to the unique microwave heating properties. In this sense, carbon materials present a high microwave absorption capacity, which could lead to the preferential/enhanced local microwave absorption features in the regions of the catalyst where carbon deposits are generated. As a consequence, local temperature deviations (hotspots) may be generated, favoring the carbon gasification by CO_2, as compared to a situation in which a constant temperature in the catalyst is held, as in the case of resistive heating. These results further confirmed the unique advantage of MW heating for DMR in facilitating coke gasification [7,15], which can minimize catalyst deactivation, ensuring a more stable operation, as shown in Fig. 5.

4. Conclusions

Nanostructured catalysts with a well-defined core-shell structure were successfully prepared by a modified Stober method followed by metal deposition. The core@shell materials, composed of β-SiC nanoparticles, with a mean particle size below 100 nm, coated by a uniform SiO_2 shell of 30 nm thickness, presented highly dispersed Rh nanoparticles with a mean particle size of 2.5 nm. These materials exhibited sufficient microwave absorption capacity so as to be heated up to the reaction temperature without the addition of another microwave absorbing material into the catalyst bed.

The Rh/SiC@SiO_2 materials were used as catalysts for the dry reforming of methane reaction, both under resistive heating and microwave heating conditions. The results showed that the operation under microwave heating conditions led to an enhancement of the reverse water gas shift reaction activity, which takes place in parallel with the dry reforming of methane process, as compared to the operation under resistive heating conditions. On the other hand, the operation under microwave heating conditions also yielded a stable operation with time on stream for the catalyst, with the suppression of irreversible coke deposition. These results clearly highlight that the engineering of catalysts in this core@shell structuration at the nanometric scale is a suitable approach for developing a catalytic system with enhanced microwave absorption properties and stability with time on stream.

CRediT authorship contribution statement

Max Caspers: Visualization, Methodology, Writing – original draft, Validation, Investigation. **José Palomo:** Writing – review & editing, Supervision, Methodology, Funding acquisition, Data curation, Writing – original draft, Project administration, Investigation, Formal analysis, Conceptualization. **Atsushi Urakawa:** Writing – review & editing, Resources, Methodology, Funding acquisition, Conceptualization, Supervision, Project administration, Investigation, Data curation.

Declaration of Competing Interest

The authors declare the following financial interests/personal relationships which may be considered as potential competing interests: Atsushi Urakawa reports financial support was provided by Japan Science and Technology Agency. Jose Palomo reports financial support was provided by European Commission. If there are other authors, they declare that they have no known competing financial interests or personal relationships that could have appeared to influence the work reported in this paper.

Acknowledgements

We thanks the financial support from the Japanese Science and Technology Agency (JST) PRESTO (Grant no. JPMJPR16S3) and from the European Union's Horizon 2020 research and innovation program under the Marie Skłodowska-Curie Grant Agreement no. 101023416 of J. Palomo.

Appendix A. Supporting information

Supplementary data associated with this article can be found in the online version at doi:10.1016/j.cattod.2025.115464.

Data availability

Data will be made available on request.

References

[1] Y. Guan, G. Song, C. Li, K.H. Lim, B. Wang, L. Xia, H. Song, Y. Liu, C. Wu, S. Kawi, Ni-based core-shell structured catalysts for efficient conversion of CH4 to H2: a review, Carbon Capture Sci. Technol. 11 (2024) 100200.
[2] R. Kaneda, J. Palomo, L. Hu, A. Urakawa, Oxidative coupling of methane under microwave: core–shell catalysts for selective C 2 production and homogeneous temperature control, Catal. Sci. Technol. 13 (2023) 5757–5766.
[3] Y. Li, G. Veser, Methane and natural gas utilization, Energy Technol. 8 (2020) 2000460.
[4] R. Franz, E.A. Uslamin, E.A. Pidko, Challenges for the utilization of methane as a chemical feedstock, Mendeleev Commun. 31 (2021) 584–592.
[5] I.E. Agency, Greenhouse Gas Emissions from Energy Data Explorer – Data Tools – IEA.
[6] C. Karakaya, R.J. Kee, Progress in the direct catalytic conversion of methane to fuels and chemicals, Prog. Energy Combust. Sci. 55 (2016) 60–97.
[7] T.P. Pham, K.S. Ro, L. Chen, D. Mahajan, T.J. Siang, U. Ashik, J.-i. Hayashi, D. Pham Minh, D.-V.N. Vo, Microwave-assisted dry reforming of methane for syngas production: a review, Environ. Chem. Lett. 18 (2020) 1987–2019.
[8] B. Fidalgo, A. Domínguez, J. Pis, J. Menéndez, Microwave-assisted dry reforming of methane, Int. J. Hydrog. Energy 33 (2008) 4337–4344.
[9] I. de Dios García, A. Stankiewicz, H. Nigar, Syngas production via microwave-assisted dry reforming of methane, Catal. Today 362 (2021) 72–80.
[10] R. Tsuchida, H. Kurokawa, T. Yamamoto, H. Ogihara, Dry reforming of methane on low-loading Rh catalysts, ChemCatChem 17 (2025) e202401386.
[11] D.S. Choi, N.Y. Kim, E. Yoo, J. Kim, J.B. Joo, Enhanced coke resistant Ni/SiO2@ SiO2 core–shell nanostructured catalysts for dry reforming of methane: effect of metal-support interaction and SiO2 shell, Chem. Eng. Sci. 299 (2024) 120480.
[12] B. Fidalgo, A. Arenillas, J. Menéndez, Mixtures of carbon and Ni/Al2O3 as catalysts for the microwave-assisted CO2 reforming of CH4, Fuel Process. Technol. 92 (2011) 1531–1536.
[13] R. Colombo, G. Moroni, C. Negri, G. Delen, M. Monai, A. Donazzi, B. M. Weckhuysen, M. Maestri, Surface carbon formation and its impact on methane dry reforming kinetics on rhodium-based catalysts by operando Raman spectroscopy, Angew. Chem. Int. Ed. 63 (2024) e202408668.
[14] J. Menéndez, A. Arenillas, B. Fidalgo, Y. Fernández, L. Zubizarreta, E.G. Calvo, J. M. Bermúdez, Microwave heating processes involving carbon materials, Fuel Process. Technol. 91 (2010) 1–8.
[15] Y. Shi, X. Tian, Z. Deng, F. Wang, Microwave catalytic dry reforming of methane over Ni/SiC catalysts for efficient syngas production, Fuel 388 (2025) 134574.
[16] A. Ramirez, J.L. Hueso, M. Abián, M.U. Alzueta, R. Mallada, J. Santamaria, Escaping undesired gas-phase chemistry: microwave-driven selectivity enhancement in heterogeneous catalytic reactors, Sci. Adv. 5 (2019) eaau9000.
[17] H.M. Nguyen, J. Sunarso, C. Li, G.H. Pham, C. Phan, S. Liu, Microwave-assisted catalytic methane reforming: a review, Appl. Catal. A 599 (2020) 117620.
[18] I. Julian, H. Ramirez, J.L. Hueso, R. Mallada, J. Santamaria, Non-oxidative methane conversion in microwave-assisted structured reactors, Chem. Eng. J. 377 (2019) 119764.
[19] L.S. Gomi, M. Afsharpour, P. Lianos, Novel porous SiO2@ SiC core-shell nanospheres functionalized with an amino hybrid of WO3 as an oxidative desulfurization catalyst, J. Ind. Eng. Chem. 89 (2020) 448–457.
[20] N.-P. Nguyen, B.-N.T. Le, T. Nguyen, T.-L.H. Duong, H.-H.T. Nguyen, D.-V.N. Vo, T.-T. Nguyen, H.-D.P. Nguyen, T.-P.T. Pham, Nickel catalyst supported on SiC incorporated SiO2 for CO2 methanation: positive effects of dysprosium promoter and microwaves heating method, Fuel 363 (2024) 130939.
[21] Y. Yin, J. Fang, Z. Qin, K. Liu, R. Yang, Toughening effect and mechanical behaviour of SiC@ SiO2 whisker-reinforced vitrified diamond composites, Int. J. Refract Met. Hard Mater. 71 (2018) 190–197.
[22] W. Stöber, A. Fink, E. Bohn, Controlled growth of monodisperse silica spheres in the micron size range, J. Colloid Interface Sci. 26 (1968) 62–69.
[23] Y. Zhang, M. Zhang, J. Yang, L. Ding, J. Zheng, J. Xu, S. Xiong, Formation of Fe 3 O 4@ SiO 2@ C/Ni hybrids with enhanced catalytic activity and histidine-rich protein separation, Nanoscale 8 (2016) 15978–15988.
[24] J. Liao, J. Qiu, G. Wang, R. Du, N. Tsidaeva, W. Wang, 3D core-shell Fe3O4@ SiO2@ MoS2 composites with enhanced microwave absorption performance, J. Colloid Interface Sci. 604 (2021) 537–549.

[25] Y. Zhang, Q. Wang, Z. Ren, Y. Yang, Preparation and characterization of mesoporous SiC/SiO2 composite nanorods, Mater. Chem. Phys. 243 (2020) 122573.
[26] Y. Liu, L. Li, S. Liu, C. Xie, S. Yu, Synthesis of silanized magnetic Ru/Fe 3 O 4@ SiO 2 nanospheres and their high selectivity to prepare cis-pinane, RSC Adv. 6 (2016) 81310–81317.
[27] S. Brunauer, P.H. Emmett, E. Teller, Adsorption of gases in multimolecular layers, J. Am. Chem. Soc. 60 (1938) 309–319.
[28] E.M. Petersen, R.G. Rao, B.C. Vance, J.-P. Tessonnier, SiO2/SiC supports with tailored thermal conductivity to reveal the effect of surface temperature on Ru-catalyzed CO2 methanation, Appl. Catal. B Environ. 286 (2021) 119904.
[29] M. Thommes, K. Kaneko, A.V. Neimark, J.P. Olivier, F. Rodriguez-Reinoso, J. Rouquerol, K.S. Sing, Physisorption of gases, with special reference to the evaluation of surface area and pore size distribution (IUPAC Technical Report), Pure Appl. Chem. 87 (2015) 1051–1069.
[30] P.N. Romano, J.F.S. de Carvalho Filho, J.M.A.R. de Almeida, E.F. Sousa-Aguiar, Screening of mono and bimetallic catalysts for the dry reforming of methane, Catal. Today 394 (2022) 348–356.
[31] S. Gaur, D.J. Haynes, J.J. Spivey, Rh, Ni, and Ca substituted pyrochlore catalysts for dry reforming of methane, Appl. Catal. A 403 (2011) 142–151.
[32] T.G. de Araújo Moreira, J.F.S. de Carvalho Filho, Y. Carvalho, J.M.A.R. de Almeida, P.N. Romano, E.F. Sousa-Aguiar, Highly stable low noble metal content rhodium-based catalyst for the dry reforming of methane, Fuel 287 (2021) 119536.
[33] S.K. Milonjić, L.S. Čerović, D.M. Čokeša, S. Zec, The influence of cationic impurities in silica on its crystallization and point of zero charge, J. Colloid Interface Sci. 309 (2007) 155–159.
[34] S. Kondo, F. Fujiwara, M. Muroya, The effect of heat-treatment of silica gel at high temperature, J. Colloid Interface Sci. 55 (1976) 421–430.
[35] D. Pinto, L. Hu, A. Urakawa, Enabling complete conversion of CH4 and CO2 in dynamic coke-mediated dry reforming (DC-DRM) on Ni catalysts, Chem. Eng. J. 474 (2023) 145641.
[36] S. Li, C. Luo, B. Robinson, J. Hu, J. Yang, Y. Wang, Production of syngas at lower temperatures through microwave-enhanced dry reforming of methane, Int. J. Hydrog. Energy 81 (2024) 187–192.
[37] D. Cao, C. Luo, Z. Tan, T. Luo, Z. Shi, F. Wu, X. Li, Y. Zheng, L. Zhang, Carbon deposition properties and regeneration performance of La2NiO4 perovskite oxide for dry reforming of methane, J. Environ. Chem. Eng. 11 (2023) 111022.
[38] K. Wittich, M. Krämer, N. Bottke, S.A. Schunk, Catalytic dry reforming of methane: insights from model systems, ChemCatChem 12 (2020) 2130–2147.